

Fe₃O₄ nanoparticle-encapsulated mesoporous carbon composite: An efficient heterogeneous Fenton catalyst for phenol degradation

Angamuthu Mani¹ · Thirumoorthy Kulandaivelu¹ · Satishkumar Govindaswamy¹ · Akhila Maheswari Mohan¹

Received: 3 April 2017 / Accepted: 27 June 2017 / Published online: 11 July 2017
© Springer-Verlag GmbH Germany 2017

Abstract Magnetite (Fe₃O₄) nanoparticle-encapsulated mesoporous carbon nanocomposite was fabricated from Fe-based metal–organic framework (MOF) (MIL-102) through carbonization. It was found that Fe-based MOF (MIL-102) is a potential precursor for the fabrication of hexagonal mesoporous carbon nanodisk functionalized with Fe₃O₄ nanoparticles. The obtained nanocomposite was characterized by XRD, FT-IR, N₂ adsorption and desorption, FE-SEM and HRTEM techniques. As a Fenton-like solid catalyst for phenol degradation, Fe₃O₄ nanoparticle-encapsulated mesoporous carbon showed greater catalytic activity for the production of hydroxyl radical from the decomposition of H₂O₂ and it accomplished 100% phenol and 82% total organic carbon (TOC) conversion, within 120 min of reaction. This enhanced catalytic performance was due to confined access for the pollutant to the iron oxide nanoparticles provided by mesopores in carbon shell. Bare Fe₃O₄ nanodisk shows poor catalytic performance in the degradation of phenol, and it obviously reveals the significance of the mesoporous carbon support for iron oxide nanoparticles.

Keywords Heterogeneous Fenton · Fe-MOF · Phenol degradation · Mesoporous carbon · Fe₃O₄ nanoparticle · AOP

Introduction

Worldwide surface water contamination is a critical environmental concern because of continuous release of polluted water by pharmaceutical, petrochemical, textile and paper industries (Santos et al. 2010). In the field of clean water production, it is a huge challenge to treat the water having trace level of refractory organic compounds (ROC). Among the ROC, phenolic compounds are classified as priority contaminant by the US Environmental Protection Agency (EPA) because of their toxicity even at very low concentration (Kavitha and Palanivelu 2016). Phenol is applied as germicidal and local anaesthetic substance, and it is also prescribed for animal's internal antiseptics and gastric anaesthetics. Coal processing unit involves the release of water containing 9–6800 mg/l of phenol; oil refineries and manufacture of petrochemicals also contaminate the water by adding phenol in 1000 mg/l (Busca et al. 2008). However, the enforced law given by EPA allows only less than 1 ppb (parts per billion) in surface waters. Deplorably, the available traditional physical, chemical and biological methods for the remediation of organic pollutants in the water claim high cost and prolonged treating time. Heterogeneous Fenton system is one of the advanced oxidation process (AOP) for the mineralization of organic pollutants in the aqueous solution by the production of oxidative hydroxyl radicals. Heterogeneous Fenton system is an upright alternative for the conventional homogeneous Fenton system where the mineralization attains only at the condition that cannot be maintained in environmental systems and it also leaves the unwanted sludge (Hartmann et al. 2010). The ultimate objective of the heterogeneous Fenton system is mineralization of organic pollutants in water at mild condition without production of secondary pollutant. However, the applied

Responsible editor: Vítor Pais Vilar

✉ Satishkumar Govindaswamy
satishkumar.g@vit.ac.in; satishgsamy@gmail.com

¹ Department of Chemistry, School of Advanced Sciences, VIT University, Vellore, Tamil Nadu 632 014, India

catalysts undergo leaching of active iron sites in the case of supported iron species and the solid iron oxide nanoparticles show lesser efficiency towards mineralization of organic pollutants due to the non-selective decomposition of hydrogen peroxide (Hartmann et al. 2010). Thus, it is still a challenge task to design heterogeneous catalyst with highly stable and active catalytic sites. Many approaches have been made to examine the catalytic activity of heterogeneous Fenton system by immobilized and substituted iron ions, iron oxide nanoparticles and iron oxide cluster on solid matrices towards mineralization of phenols (Martínez et al. 2007; Melero et al. 2006, 2007; Nidheesh 2015).

Several improvements of catalytic performance and stability of catalytic sites were examined by a supporting catalyst in the porous solid support (Li et al. 2016; Satishkumar et al. 2013; Zhou et al. 2014). Activation of catalytic sites by Cu^{2+} complex with the suitable ligands (Lyu et al. 2015) and increase of Fe^{2+} content by the partial pyrolysis of $\text{Fe}_3\text{O}_4@g\text{-C}_3\text{N}_4$ composite (Luo et al. 2016) were implemented in order to enhance the catalytic degradation of organic pollutants in water. Single-site iron catalyst has been applied to prevent leaching of ions during the catalytic degradation of organic pollutants (Zhang et al. 2015). Oxalic acid-treated Fe-silicate for the degradation of EDTA (Sashkina et al. 2016), hydrophilic modification of carbon support of the catalyst (Zheng et al. 2015) and morphology-driven Fenton catalyst (Datta et al. 2016) are some of the recent developments of heterogeneous Fenton catalyst. FeOCl supported on SBA-15 creates thin-film surface around the catalytic sites; thereby, it reduces the scavenging of hydroxyl radicals and increases the catalytic activity (Yang et al. 2015). These successfully applied catalysts were able to perform only in the limited period of time in batch reactors. In order to develop the catalysts with greater performance and prolonged stability, heterogeneous catalysts are also applied in fluidized bed, packed bed and membraned reactors (Duarte et al. 2013; Martínez et al. 2017; Satishkumar et al. 2013; Wang et al. 2016). However, the demonstrated high catalytic performance retained for short period of time due to leaching of catalytic sites. Hence, construction of specific nanostructure is one of the several recent approaches made to enhance the catalytic performance of iron-based catalyst in Fenton system. Li et al. (2015a) prepared a $\text{Fe}_2\text{O}_3@C$ core-shell by the coating of carbon on the surface of Fe_2O_3 nanoparticles, and it increases the number of active sites on the surface of Fe_2O_3 nanoparticles. Spindle of Fe_2O_3 nanoparticles and Au nanoparticles was established in mesoporous silica for the fabrication of multi-yolk-shell structure, and it displays a non-contact synergetic effect for the efficient removal of methylene blue (Chen et al. 2016). The confined space in the yolk-shell structure

composed of $\text{Fe}_3\text{O}_4@Fe_3O_4/C$ improved the catalytic degradation of 4-chlorophenol (Zeng et al. 2014). Li et al. (2015b) utilized the confined environment provided by the mesopores of SBA-15 in $\text{Fe}/\text{Pd}@SBA-15$ to enhance the catalytic performance towards degradation of Acid Red 73. However, in the case of yolk- or core-shell nanoarchitectures, metal oxide core nanoparticles encapsulated with the shell support cannot be accessed easily by reactant molecules. Thus, shells decorated with pores have gained attention in the field of catalysis.

Metal-organic frameworks (MOFs) is a new type of crystalline porous materials have gained great attention in various fields such as separation, gas storage, catalysis, chemical sensors and drug delivery (Torad et al. 2014; Liu et al. 2015). MOF provides the efficient dispersion of catalytic sites with controlled size and composition. Moreover, it provides inbuilt catalyst system for the carbonization process and it could be a single precursor for defined formation of iron oxide carbon nanocomposites. Iron oxide nanoparticles-supported carbon nanocomposites prepared from Fe-MOF are widely applied as heterogeneous Fenton system because of stabilization of metal oxide nanoparticles provided by carbon (Banerjee et al. 2012; Hao et al. 2014; Lee et al. 2014; Ribeiro et al. 2016). MOF is an excellent source for carbon than the precursors applied in the previous methods. Carbonization of MOF produces metal oxide nanoparticles and carbon matrix. At certain carbonization temperature, the formed metal oxide nanoparticles undergo carbothermal reduction by the consumption of carbon around the iron oxide nanoparticles; thereby, pores are generated in the carbon matrix. Formed pores in the carbon matrix around iron oxide nanoparticles provide the accessibility to reach catalytic sites. Fe-MIL (102) is a coordination polymer formed from Fe^{2+} and naphthalene tetra carboxylate ligand having micropores with the low surface area (Su et al. 2012). Recently, we synthesized the Fe_3O_4 nanoparticle-encapsulated mesoporous carbon composite from Fe-MIL (102) as a precursor (Angamuthu et al. 2017). Herein, we report the catalytic activity of $\text{Fe}_3\text{O}_4@mesopore$ carbon shell nanocomposite as heterogeneous Fenton catalyst towards degradation of phenol. The mesoporous carbon support prevents the aggregation of iron oxide nanoparticle, and it also provides confined access of iron oxide nanoparticles in order to prevent the non-selective decomposition of hydrogen peroxide. To evaluate the importance of porous carbon support for iron oxide nanoparticles, bare Fe_3O_4 nanoparticles are prepared by burning carbon in air and it is applied in the degradation of phenol. The influence of oxalic acid, a stable intermediate formed during the oxidation of phenol, over $\text{Fe}_3\text{O}_4@mesopore$ carbon shell nanocomposite is also investigated.

Materials and methods

Chemicals

Ferrous sulphate ($\text{FeSO}_4 \cdot 7\text{H}_2\text{O}$) (99.5%), sodium hydroxide (98%), hydrochloric acid (35%) and phenol (AR) were acquired from SRL. 1,4,5,8-Naphthalenetetracarboxylic dianhydride (NTCDA) (97%), orthophosphoric acid (99%) and catechol (99%) were bought from Alfa Aesar. Hydrogen peroxide (30% in H_2O) and acetonitrile (HPLC grade) were procured from Merck. Oxalic acid (99%) and fumaric acid (99%) were acquired from Sigma-Aldrich. All the chemicals were used without further purification.

Synthesis of Fe-MOF

Fe-MOF was synthesized by following the procedure reported in the literature (Su et al. 2012). 1,4,5,8-Naphthalenetetracarboxylic dianhydride (0.025 mmol) was dissolved in 25 ml of 0.002-M NaOH solution in 50-ml beaker. $\text{FeSO}_4 \cdot 7\text{H}_2\text{O}$ (0.05 mmol) is entirely dissolved in 5 ml water. These two solutions are mixed and stirred for 30 min at room temperature to get the homogeneous solution, it is transferred to a polypropylene bottle, and it was maintained at 60 °C for 24 h in a hot-air oven. Afterwards, the resultant precipitate was separated by centrifugation. The obtained product was washed with distilled water and then dried at hot-air oven.

Preparation of Fe-HCNA300

Fe-hexagonal, carbon matrix, nitrogen atmosphere, and air treated at 300 °C (HCNA300) is prepared by following the synthesis procedure reported in the literature (Angamuthu et al. 2017). Fe-MOF was calcined in a tubular furnace at 725 °C with the heating rate of 5 °C/min in nitrogen atmosphere and maintained for 30 min at the final temperature. The obtained sample is brought to the room temperature in nitrogen atmosphere. Then, the sample is treated at 300 °C under air atmosphere for 2 h with the heating rate of 5 °C/min to obtain Fe-HCNA300.

Catalytic studies

In a 250-ml reagent bottle, 100 ml of 200-ppm phenol solution and 50 mg of Fe-HCNA300 catalyst were taken. The required pH of the solution was adjusted with dilute hydrochloric acid and sodium hydroxide. The temperature of the reaction medium was maintained in oil bath equipped with thermocouple, and the pH of the solution was monitored using a pH electrode. Before the initiation of catalytic performance, 30 min of adsorption and desorption was allowed to attain equilibrium. It was found that 5% phenol has been adsorbed in 30 min and

further increase of contact time does not increase the phenol adsorption. Following that, defined amount of H_2O_2 was added and the samples are taken in specific interval of time. In order to quench the radicals, one drop of 1 M sodium hydroxide solution was added. Samples are filtered using nylon 66 membrane with 0.2- μm pore size to remove the catalyst before further analysis of the samples. For the recycle study, catalyst was separated with external magnetic field, washed and dried overnight in a hot-air oven for the next cycle.

Analysis

Thermogravimetric analysis (TGA) of Fe-MOF was performed at the heating rate of 5 °C/min under nitrogen atmosphere using a TA Q600 SDT instrument. The crystalline phase of Fe-MOF and Fe-HCNA300 was determined through a Bruker, D8 X-ray diffractometer, Cu $K\alpha$ radiation; the applied accelerating voltage was 30 kV and 40-mA current. The diffraction angle 2θ values are from 10° to 80° with a step size of 0.02°/min. The specific surface area, pore volume and pore size distribution of the materials (Fe-MOF, Fe-HCNA300) were characterized by BET methods and Barrett–Joyner–Halenda (BJH) methods using a Micromeritics ASAP 2020 instrument at 77 K. The surface morphology of Fe-HCNA300 was acquired by field emission scanning electron microscope (FE-SEM) (Supra 55 Carl Zeiss equipped with Oxford X-act energy-dispersive spectrometer (EDS)). High-resolution transmission electron microscope (HRTEM) image of Fe-HCNA300 was obtained through a JEOL JEM 2100 instrument. FT-IR spectra of Fe-MOF and Fe-HCNA300 were recorded in the range of 4000–400/cm using a Shimadzu IR Affinity-1 instrument equipped with a high-sensitivity DLATGS detector. A TOC-L Shimadzu instrument was used to determine the amount of total organic carbon present in the treated water sample through the NPOC method. The leached iron ions were detected using an atomic absorption spectrometer (AAS), Varian AA240. Intermediates from degradation of phenol were identified using HPLC (JASCO LC 4000). C18 reversed-phase column was used with methanol and water (50:50) as the mobile phase.

Results and discussion

Physicochemical characterization of catalytic materials

The X-ray diffraction pattern of as-synthesized Fe-MOF is shown in Fig. 1(a), which obviously expresses a crystalline structure, and the major diffraction peaks observed at the 2θ values between 20° and 50° are indexed to Fe-MOF (MIL-102) without any additional diffraction peaks (Su et al. 2012). The recorded N_2 adsorption and desorption isotherm (Fig. 2(a)) and pore size distribution of Fe-MOF shown in Fig.

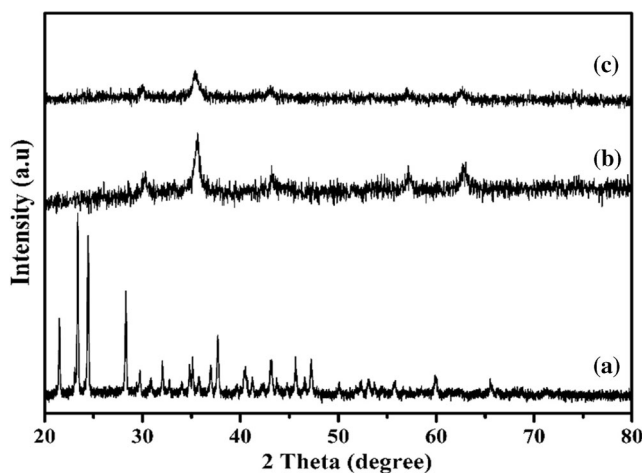


Fig. 1 Powder X-ray diffraction pattern of *a* Fe-MOF, *b* Fe-HCNA300 and *c* Fe-HCNA300 after three catalytic cycles

3(a) endorse the microporous nature of the as-prepared Fe-MOF. It is further supported by the measured very low pore volume ($0.019 \text{ cm}^3/\text{g}$) of Fe-MOF with the surface area of $60.363 \text{ m}^2/\text{g}$. The presence of absorption band at $1609/\text{cm}$ for coordinated C=O groups and the absence of absorption band for uncoordinated C=O groups at $1730/\text{cm}$ in the FT-IR spectra (Fig. 4(a)) of as-synthesized Fe-MOF confirm the coordination of iron ions and NTCDA ligand. The transformation of Fe-MOF to carbon-based heterogeneous Fenton catalyst was performed by carbonization of Fe-MOF under N_2 atmosphere at various temperatures. In order to observe the applicable temperature for the calcination of Fe-MOF, TGA was carried out under the nitrogen atmosphere. Thermogram (Fig. 5) of Fe-MOF displays the thermal decomposition of Fe-MOF under the nitrogen atmosphere. The weight loss observed up to $220 \text{ }^\circ\text{C}$ (19.8%) is due to the departure of water molecules adsorbed at the micropores of Fe-MOF. The weight loss perceived from 230 to $380 \text{ }^\circ\text{C}$ (39.47%) is because of the decomposition of naphthalene tetra carboxylate ligand of the Fe-MOF. The 15.6% weight loss observed near 700 to $780 \text{ }^\circ\text{C}$ is crucial for the catalytic graphitization. Active composition, size of catalytic sites and the generation of mesopores in the carbon framework could be improved by carbonization time and temperature. Amorphous carbon encapsulated around the Fe_3O_4 nanoparticles is graphitized into crystalline carbon by the reduction of Fe_3O_4 nanoparticles into $\alpha\text{-Fe}$ (Maldonado-Hódar et al. 2000; Lei et al. 2007; Tang et al. 2013), and this process generates the mesopores in the carbon framework. Based on TGA results, $725 \text{ }^\circ\text{C}$ was chosen as the optimum temperature for the carbonization of Fe-MOF towards fabrication of iron oxide nanoparticle-embedded mesoporous carbon. However, the existence of $\alpha\text{-Fe}$ in the heterogeneous Fenton systems leads to leaching of iron ions due to the attack of acidic intermediates formed in the course of degradation. Hence, calcined material derived at $725 \text{ }^\circ\text{C}$ was exposed into $300 \text{ }^\circ\text{C}$ heat treatment

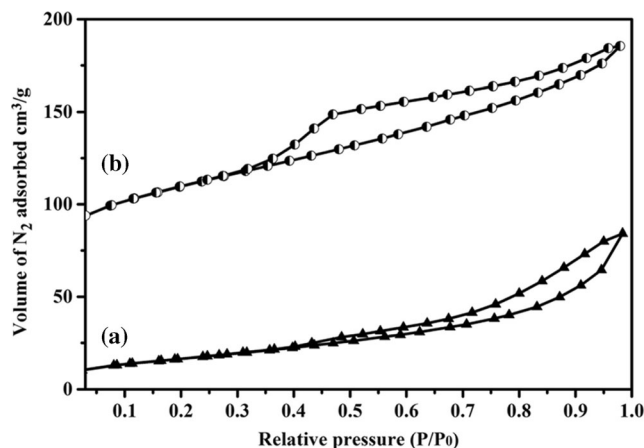


Fig. 2 N_2 adsorption and desorption isotherm of *a* Fe-MOF and *b* Fe-HCNA300

under air atmosphere for the conversion of $\alpha\text{-Fe}$ to the Fe_3O_4 nanoparticles (Angamuthu et al. 2017). It was observed and accepted that the composition and morphology of the carbon source define the morphology and structure of the resulting carbon material (Wei et al. 2015). Hence, it is anticipated that the resulting carbon materials would possess the hexagonal morphology of Fe-MOF. Accordingly, the calcined material is termed as Fe-HCNA300. X-ray diffraction patterns of Fe-HCNA300 shown in Fig. 1(b) denote the planes of Fe_3O_4 nanoparticles (220), (311), (400), (422), (511) and (440) with the 2θ values of 30.0° , 35.5° , 43.2° , 53.8° , 57.2° and 62.6° (JCPDS No. 65-3107). There are no corresponding peaks for $\alpha\text{-Fe}$, and it confirms the complete conversion of $\alpha\text{-Fe}$ into Fe_3O_4 nanoparticles during the $300 \text{ }^\circ\text{C}$ air treatment. Moreover, the obtained X-ray diffraction pattern resembles with the previous literature (Angamuthu et al. 2017). Scherer's equation was applied to define the size of catalytic site (Fe_3O_4) dispersed in carbon matrix during the carbonization, and the result shows that Fe-HCNA300 was dispersed with 20 nm of Fe_3O_4 nanoparticles. The N_2 adsorption and desorption isotherm of Fe-HCNA300 shown in Fig. 2(b) is a typical type IV isotherm, and the hysteresis loop at the high

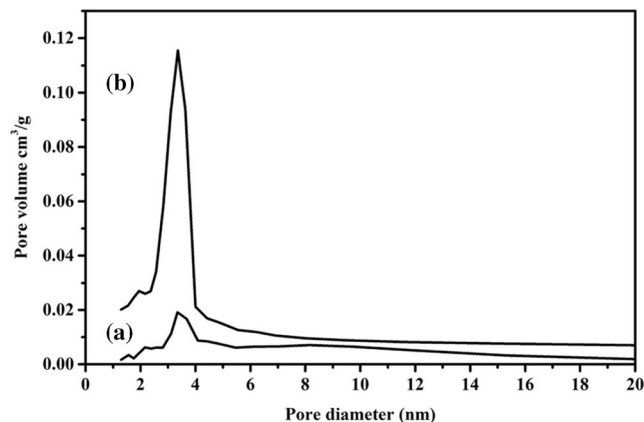


Fig. 3 BJH pore size distribution of *a* Fe-MOF and *b* Fe-HCNA300

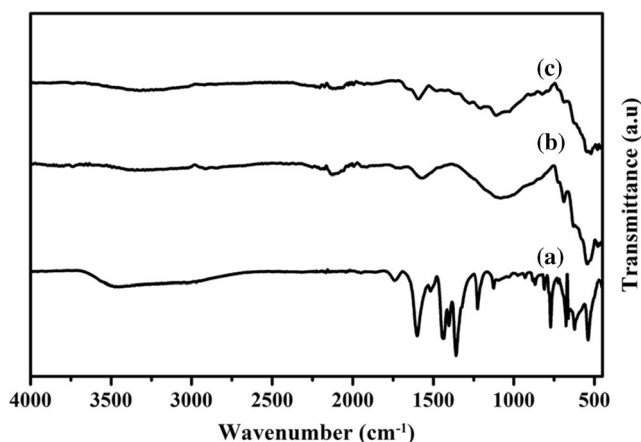


Fig. 4 FT-IR spectra of *a* Fe-MOF, *b* Fe-HCNA300 and *c* Fe-HCNA300 after three catalytic cycles

relative pressure validates the presence of mesopores in Fe-HCNA300. The peak centred at 3.36 nm in the BJH pore size distribution of Fe-HCNA300 shown in Fig. 3(b) endorses the mesoporous nature of Fe-HCNA300. The carbothermal reduction and escape of residues in the carbon framework during the air treatment have increased the surface area to 212.6 m²/g with the pore volume of 0.11 cm³ compared to Fe-MOF. Low-angle XRD pattern (not provided) of Fe-HCNA300 explains that there are no diffraction peaks for ordered pore structure. Thus, formed mesopores during the carbonization of Fe-MOF are disordered and open to access. The recorded FT-IR spectra of Fe-HCNA300 shown in Fig. 4(b) describe the stretch of Fe–O bond in Fe₃O₄ nanoparticles around 547/cm, and it further supports the presence of Fe₃O₄ in Fe-HCNA300. FE-SEM of image Fig. 6a shows the well-defined uniform shape with evenly dispersed hexagonal particles of Fe-HCNA300. During the thermal treatment, there is no distortion in porous network of carbon structure and it is confirmed by FE-SEM image. The recorded EDAX pattern for the selected area provides composition (25.45 wt% carbon and 36.7 wt% iron) of Fe-HCNA300. The porous nature of Fe-HCNA300 further is revealed by HRTEM image displayed in Fig. 6b. Both FE-SEM and HRTEM declare that the carbonized products recovered the inherited morphology of Fe-MOF. The composition and structural features of Fe-HCNA300 were explored in our previous report (Angamuthu et al. 2017).

Performance of catalyst towards degradation of phenol

A series of contrast experiments were implemented for the investigation of catalytic performance of Fe-HCNA300 as a heterogeneous Fenton catalyst towards degradation of phenol. The experiments were divided into three parts. The first part investigates the influence of reaction conditions such as initial hydrogen

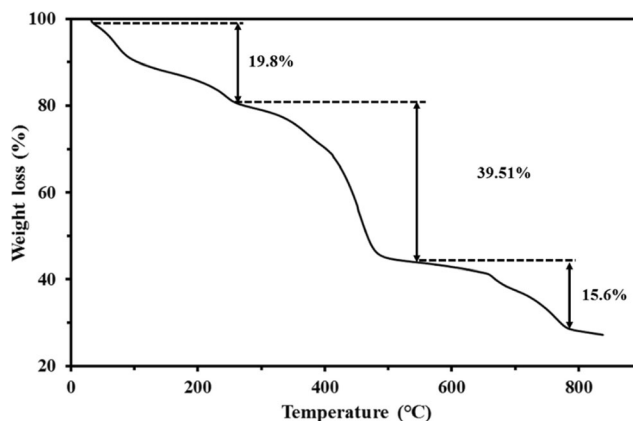


Fig. 5 Thermogravimetric analysis of Fe-MOF under N₂ atmosphere

peroxide concentration, initial pH of the solution, temperature and time. The stability and recyclability of Fe-HCNA300 were explored in the second part. Intermediates produced during the Fenton oxidation of phenol and the influence of oxalic acid (stable and acidic intermediate formed from the degradation of phenol) were observed in the third part of the study.

Effect of hydrogen peroxide

Hydrogen peroxide (H₂O₂) is a source for hydroxyl radical formation, and its concentration influences the efficiency of the phenol mineralization in the Fenton reaction. Fourteen moles of H₂O₂ is a theoretical requirement for the complete mineralization of 1 mol of phenol (Liao et al. 2009). Therefore, in our case, 200 mg/l of 100 ml phenol solution requires 2.97 mmol of H₂O₂. The effect of initial hydrogen peroxide (H₂O₂) dosage on the degradation of phenol was investigated by increasing the concentration of hydrogen peroxide from 2.97 to 4.158 mmol, and the obtained results are shown in Fig. 7a. It could be seen that increase of H₂O₂ dosage results only in marginal effect on total organic carbon (TOC) conversion. H₂O₂ dosage of 4.158 mmol achieved around 85% of TOC conversion within 120 min of degradation reaction and in the case of 3.56 mmol demonstrated 82% of TOC. It is interesting to note that after 120 min of reaction, 2.97 mmol of H₂O₂ (stoichiometric) is able to show 80% TOC conversion and the remaining 20% TOC is responsible for the biodegradable carboxylic acid intermediates such as formic, acetic and oxalic acids. Based on the economic and TOC removal performance, 2.97 mmol (stoichiometric) is preferred as the H₂O₂ concentration for further studies. The observed 80% TOC conversion highlights the 80% H₂O₂ efficiency towards production of OH radicals. The increase of H₂O₂ dosage increased leached iron concentration from 7 (3.8%) to 10 ppm (5.6%) (Fig. 7a). However, the contribution of leached iron ions towards homogeneous Fenton reaction is negligible, since it does not meet the minimum requirement of iron ion concentration.

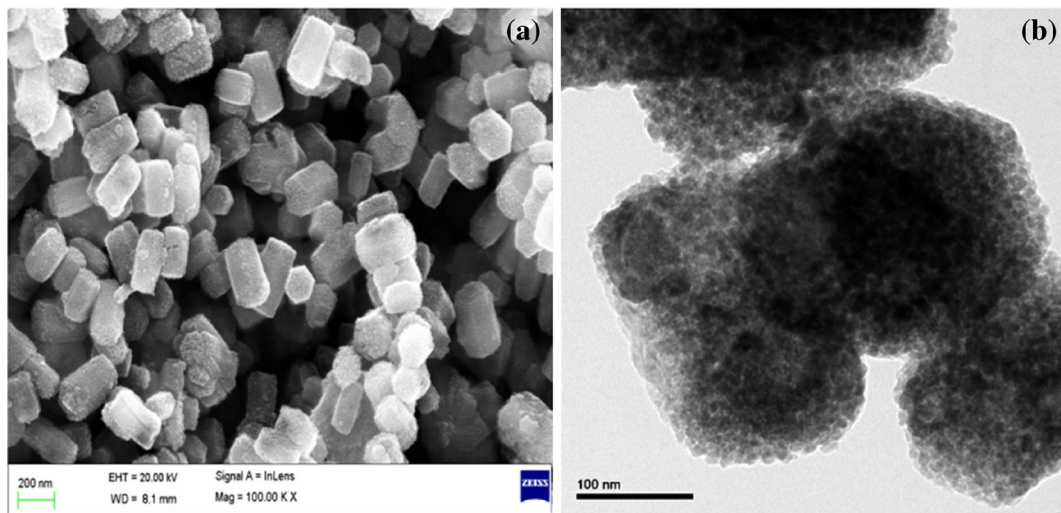


Fig. 6 Fe-HCNA300. **a** FE-SEM. **b** HRTEM

Effect of temperature

The degradation of phenol was executed at the temperatures between 40 and 80 °C to assess the influence of

temperature on the degradation of phenol involving Fe-HCNA300 as catalyst, and the observed results are shown in Fig. 7b. The degree of mineralization of phenol improved with the increase of temperature. The surge of

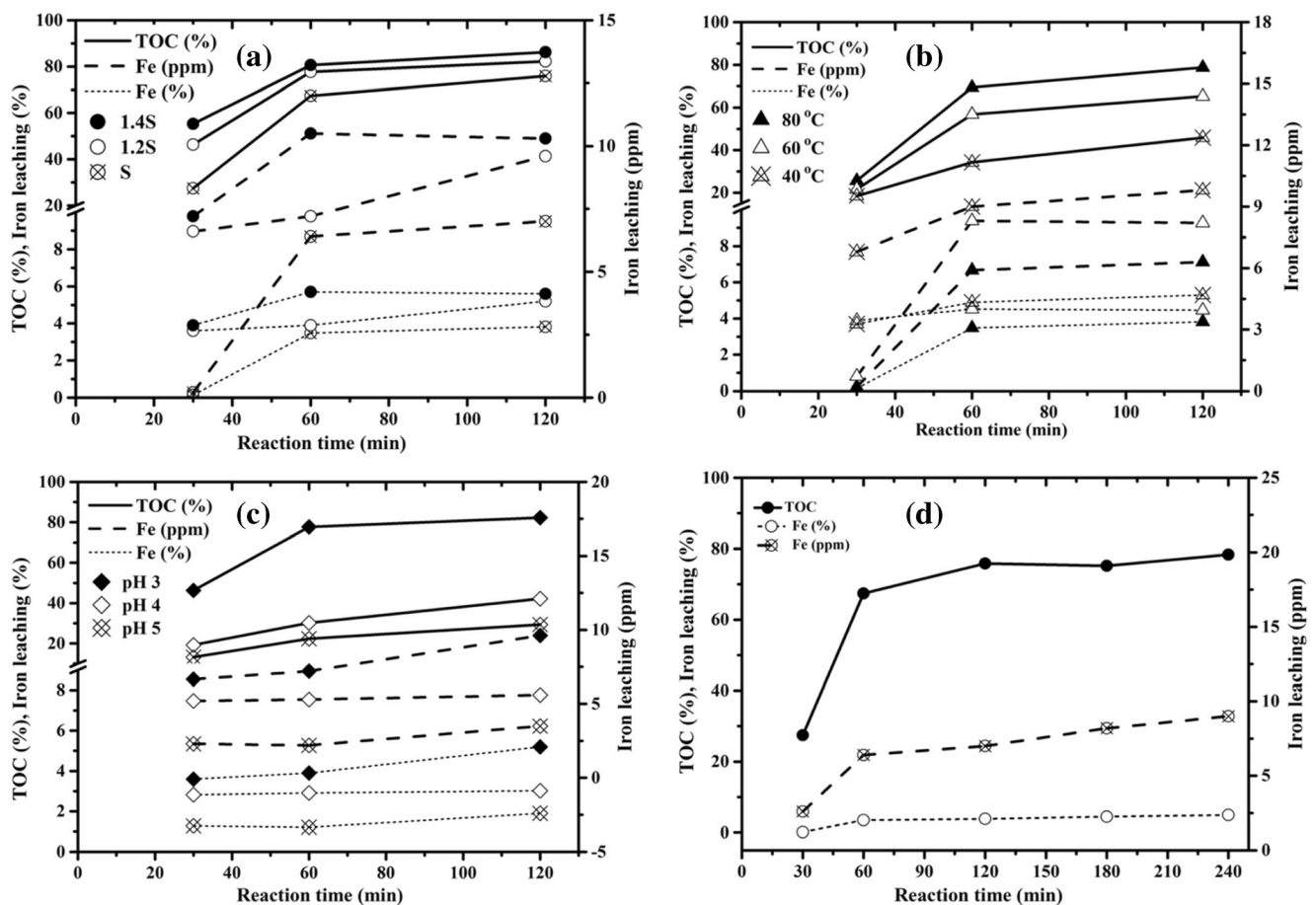
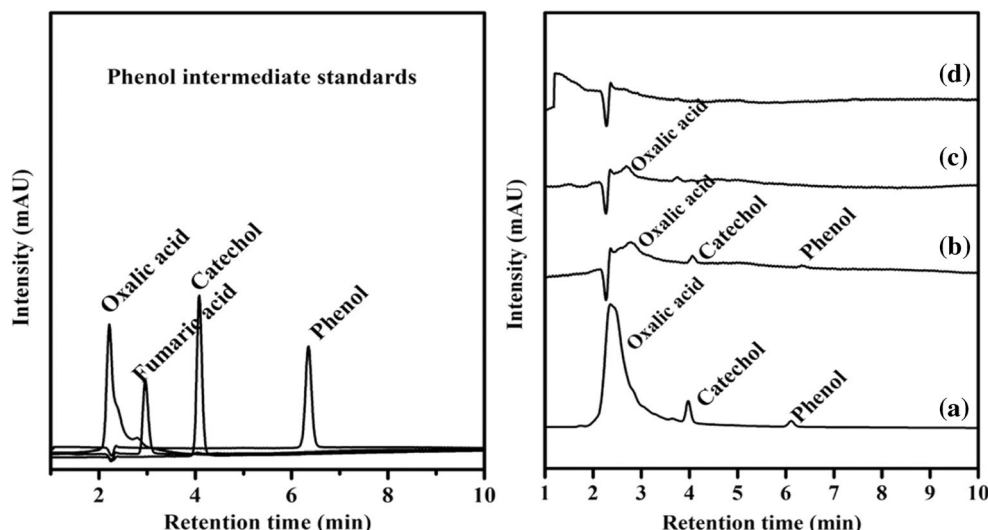


Fig. 7 Optimization of operation conditions for 100 ml of 200 ppm phenol degradation over 50 mg of Fe-HCNA300. **a** Effect of hydrogen peroxide concentration (pH = 3, 80 °C). **b** Effect of temperature (pH = 3,

stoichiometric H₂O₂). **c** Effect of pH (80 °C, stoichiometric H₂O₂). **d** Effect of time (stoichiometric H₂O₂, pH = 3, 80 °C) (S stoichiometric)

Fig. 8 HPLC chromatogram of phenol conversion and its intermediates at *a* 15, *b* 30, *c* 60 and *d* 120 min

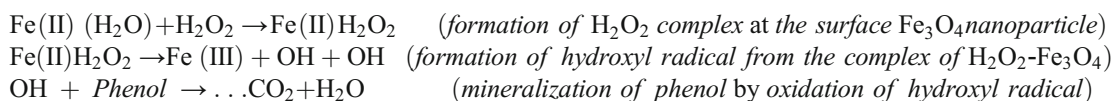


temperature from 40 to 80 °C drastically raises TOC conversion from 45 to 79% within 120 min of the reaction time with 3.82% of Fe leaching. The decline of TOC conversion (40%) was observed while dropping the temperature to 40 °C is due to the reduction in ·OH radical production. Rate constants for hydroxyl radical formation and Fe³⁺/Fe²⁺ redox cycle are exponentially related with temperature. Thus, the rate of the mineralization reaction increases while increasing the temperature of the reaction medium. Rising of temperature above 90 °C leads to the non-selective thermal decomposition of H₂O₂, which

leads to less efficiency (Herney-Ramirez et al. 2008; Melero et al. 2007). Hence, 80 °C is chosen as an optimum temperature for the degradation of phenol.

Effect of pH

Initial solution pH has a significant influence on H₂O₂ towards hydroxyl radical formation. As per mechanism proposed by Lin and Gurol (1998), hydroxyl radicals are generated from H₂O₂ at the surface of the Fe₃O₄ nanoparticles as follows:



The above equations describe the requirement of protons for the formation of hydroxyl radical by the catalytic decomposition of hydrogen peroxide. The role of pH on the

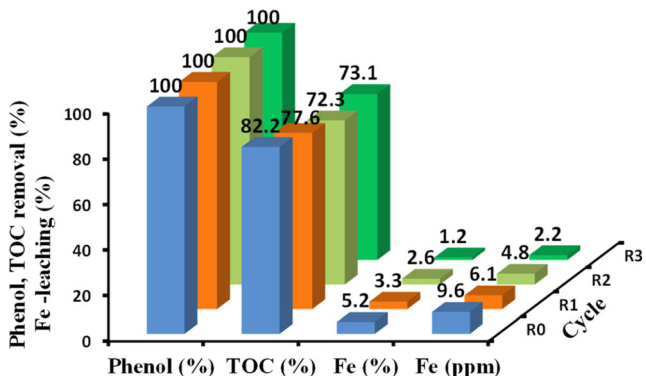


Fig. 9 Recycle study of Fe-HCNA300 towards degradation of phenol (50 mg Fe-HCNA300, 200 ppm of phenol, H₂O₂ (stoichiometric), 80 °C, 120 min)

degradation of phenol was studied with three different pH values varying from 3 to 5, and the catalytic results are shown in Fig. 7c. Higher catalytic performance 82% of TOC conversion was accomplished at pH 3, and the further increase of pH to 4 lowers the catalytic performance to 42% TOC conversion. While, at pH 5, only 29% TOC conversion was detected. The observation of lowering catalytic performance with increasing of pH value is distinctive of Fenton reaction as referred from literature (Herney-Ramirez et al. 2008).

Effect of reaction time

The degradation of phenol is monitored with the TOC conversion at different reaction times (Fig. 7d). It is observed that an increase of reaction time beyond 120 min does not improve the TOC conversion. It is interesting to note that 65% of mineralization was achieved within 60 min of the reaction; however, it takes additional 60 min to reach the 76% of TOC

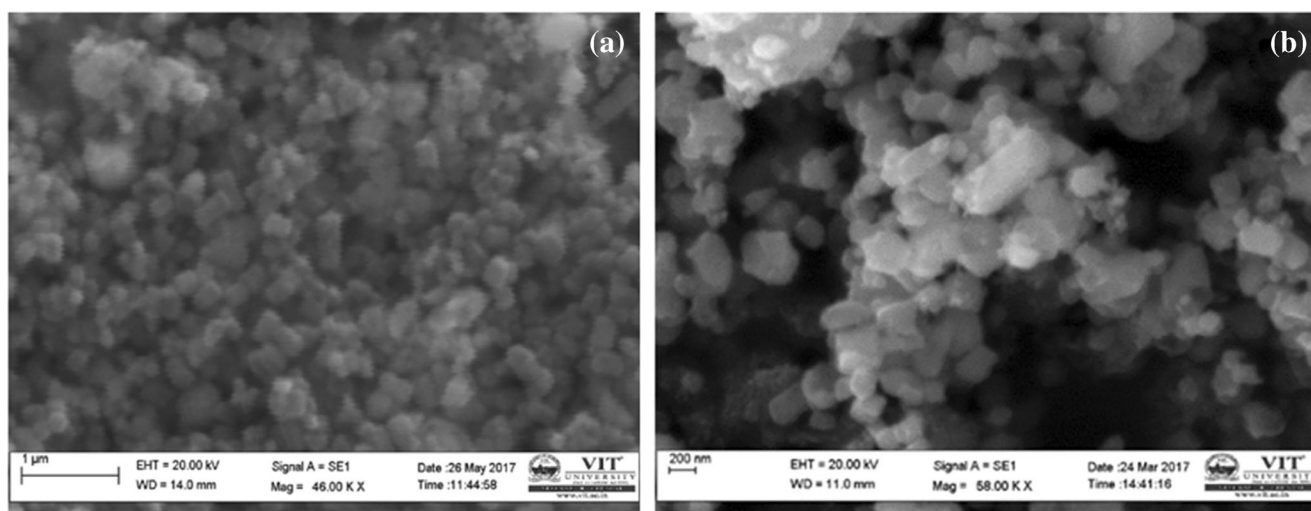


Fig. 10 SEM image of **a** Fe-HCNA300 after 3 cycles and **b** Fe₃O₄ nanodisk derived from Fe-HCNA300

conversion. It is due to the formation of robust intermediates during the course of reaction. HPLC analysis (Fig. 8) was applied to monitor the conversion of phenol during the oxidation and identification of intermediates formed. It could be seen that the presence of phenol at trace level in the samples recovered at 30 min. However, peak for phenol is not observed in the HPLC chromatogram of the sample collected after 60-min reaction. This observation endorses higher catalytic activity of Fe-HCNA300 towards phenol conversion. HPLC chromatogram further suggests that the major intermediates formed within 15 min of reaction, and it required 120 min to reach the negligible concentration (Fig. 8). Thus, 120 min was chosen as the preferred reaction time for the degradation of phenol. The enrichment of degradation products in the mesoporous channels of Fe-HCNA300 creates a concentration gradient, which increases diffusion of reactant molecules through mesopore channels to reach catalytic sites.

Recyclability and stability of Fe-HCNA300

Recyclability of Fe-HCNA300 catalyst was tested at the optimized condition. After the completion of each run, external

magnetic field is applied to recover the catalyst from the reaction medium. Before the use of the catalyst for the next cycle, the catalyst was repeatedly washed with ethanol in order to remove the adsorbed phenol and its intermediates on the surface of the catalyst and then the catalyst was dried in a hot-air oven at 100 °C overnight. Figure 9 shows the results of the recycle test of Fe-HCNA300 towards mineralization of phenol (200 mg/l 100 ml of phenol, 2.97 mmol of H₂O₂, pH 3, 2 h and 80 °C). The Fe-HCNA300 catalyst shows persistent results with high TOC conversion. The dissolution of percentage of iron ions into the reaction medium gradually decreases to 1.2%. The FT-IR spectra of fresh Fe-HCNA300 and spent catalyst that has performed 3 cycles resemble with the fresh Fe-HCNA300 (Fig. 4). It demonstrates that the catalytic active and carbon support did not undergo any change during the catalytic performance. It is additionally supported by X-ray diffraction pattern of spent Fe-HCNA300 (Fig. 1(c)), and there is no change in diffraction pattern after three catalytic cycles. The SEM image (Fig. 10a) confirms that the majority of Fe-HCNA300 retained hexagonal morphology after three catalytic performances. The above catalytic performance and characterization results of spent catalyst describe the stable structure of Fe-HCNA300.

Table 1 Comparison of phenol degradation over Fe-HCNA300 with other catalysts under similar reaction conditions

Catalyst (weight)	Phenol (ppm)/ volume	Time (min)	Temp. (°C)	pH	H ₂ O ₂	Fe (wt%)	Phenol (%)	TOC (%)	Fe leaching (ppm)	References
Fe/ZSM (1.5 g/l)	0.069 mol (–)	180	70	3.5	1.5 S	–	100	46	3.7	Fajerwerg and Debellefontaine (1996)
Fe/AC (0.5 g/l)	100 (50 ml)	240	50	3	S	4	100	84	2.4	Zazo et al. (2006)
Fe ₃ O ₄ (5 g/l)	4700 (20 ml)	360	35	6	86 S	–	100	42.7	<1	Zhang et al. (2009)
Fe ₃ O ₄ (0.25 g/l)	600 (100 ml)	90	25	4	0.45 S	–	92	67	<1	Hou et al. (2014)
Fe-HCNA300 (0.5 g/l)	200 (100 ml)	120	80	3	S	36	100	82	6.3	This work

(–) Not reported, *S* stoichiometric

Degradation of oxalic acid

Several aromatic ring compounds and short organic compounds are observed as intermediates during the Fenton degradation of phenol. Hydroquinone; catechol; and p-benzoquinone maleic, oxalic, acetic and formic acids were identified as intermediate products during the course of phenol degradation (Zazo et al. 2005). Among the observed phenol intermediates, oxalic and acetic acids are fairly refractory to oxidation. Acetic acid degradation was examined using ZSM-5 catalysts (Cihanoğlu et al. 2015), and they achieved 50.5% of COD removal. The consequence of oxalic acid on the degradation of phenol was studied by Nakagawa and Yamaguchi (2012), and they conclude that degradation efficiency of Fenton reaction obstructs by formation of excess oxalic acid and suppression of reduction of Fe^{3+} ion by coordination. Here, Fe-HCNA300 was applied to assess the catalytic performance in the degradation of recalcitrant oxalic acid (50 ppm) at the optimized condition with stoichiometric amount of H_2O_2 . The recalcitrant nature of oxalic acid for the mineralization is evident from the observation of 15% of TOC conversion. This illustrates that the degradation of phenol over Fe-HCNA300 was predominantly progressed through malonic acid intermediate, which attains the mineralization via formic acid, acetic acid and oxalic acid (Zazo et al. 2005).

Fe_3O_4 nanodisk for the degradation of phenol

Fe-HCNA300 demonstrated high catalytic activity in the degradation of phenol due to the mesopores in the carbon shell, which provides confined space to access core catalytic site Fe_3O_4 nanoparticles. In order to ascertain the role of confined space provided by mesopore in the carbon shell of Fe-HCNA300, it was calcined under the air atmosphere at 550 °C to form bare Fe_3O_4 . The SEM image of Fe-HCNA300 after calcination confirms the bare Fe_3O_4 having hexagonal nanodisk morphology (Fig. 10b). The obtained bare Fe_3O_4 nanodisks were applied in the degradation of phenol under the optimized condition. After 10 h of reaction, the maximum TOC conversion observed was only 23%. This poor performance of Fe_3O_4 nanodisk is due to non-selective decomposition of H_2O_2 and the absence of mesopore by iron oxide agglomeration. Table 1 correlates the catalytic performance of Fe-HCNA300 in the degradation of phenol with the reported catalysts in the literature. The results suggest the comparable high catalytic performance of Fe-HCNA300 towards degradation of phenol.

Conclusion

The synthesis of mesoporous carbon nanocomposites dispersed with Fe_3O_4 nanoparticles was achieved by

optimization of calcination temperature and time of Fe-based MOF. The characterization results evidence the formation of mesopores in the carbon matrix and the efficient dispersion of Fe_3O_4 nanoparticles. It demonstrated that the Fe-MOF is a prospective precursor for the fabrication of Fe_3O_4 -functionalized porous nanocomposite in a single step. The prepared solid Fenton catalyst demonstrated enhanced catalytic activity in terms of phenol and TOC conversion with less leaching of iron ions. The recycle test of Fe-HCNA300 exhibits the greater stability and activity, suggesting that Fe-HCNA300 can be applied towards degradation of ROC such as bisphenol, chlorophenol and its robust intermediates. Fe-HCNA300 can be a promising alternative for the available solid Fenton catalysts, and it could be applied in the large-scale wastewater remediation process.

Acknowledgments The authors are grateful to thank for the financial support from DST-SERB Fast Track (SR/FT/CS-138/2011) Government of India, New Delhi.

References

- Angamuthu M, Satishkumar G, Landau MV (2017) Precisely controlled encapsulation of Fe_3O_4 nanoparticles in mesoporous carbon nanodisk using iron based MOF precursor for effective dye removal. *Micropor Mesopor Mater* 251:58–68. doi:10.1016/j.micromeso.2017.05.045
- Banerjee A, Gokhale R, Bhatnagar S, Jog J, Bhardwaj M, Lefez B, Hannover B, Ogale S (2012) MOF derived porous carbon- Fe_3O_4 nanocomposite as a high performance, recyclable environmental superadsorbent. *J Mater Chem* 22:19694–19699. doi:10.1039/c2jm33798c
- Busca G, Berardinelli S, Resini C, Arrighi L (2008) Technologies for the removal of phenol from fluid streams: a short review of recent developments. *J Hazard Mater* 160:265–288. doi:10.1016/j.jhazmat.2008.03.045
- Chen Z, Liang Y, Hao J, Cui ZM (2016) Noncontact synergistic effect between Au nanoparticles and the Fe_2O_3 spindle inside a mesoporous silica shell as studied by the Fenton-like reaction. *Langmuir* 32:12774–12780. doi:10.1021/acs.langmuir.6b03235
- Cihanoğlu A, Gündüz G, Dükkanlı M (2015) Degradation of acetic acid by heterogeneous Fenton-like oxidation over iron-containing ZSM-5 zeolites. *Appl Catal B Environ* 165:687–699. doi:10.1016/j.apcatb.2014.10.073
- Datta KJ, Gawande MB, Datta KKR, Ranc V, Pechousek J, Krizek M, Tucek J, Kale R, Pospisil P, Varma RS, Asefa T, Zoppellaro G, Zboril R (2016) Micro-mesoporous iron oxides with record efficiency for the decomposition of hydrogen peroxide: morphology driven catalysis for the degradation of organic contaminants. *J Mater Chem A* 4:596–604. doi:10.1039/c5ta08386a
- Duarte F, Morais V, Maldonado-Hódar FJ, Madeira LM (2013) Treatment of textile effluents by the heterogeneous Fenton process in a continuous packed-bed reactor using Fe/activated carbon as catalyst. *Chem Eng J* 232:34–41. doi:10.1016/j.cej.2013.07.061
- Fajerweg K, Debellefontaine H (1996) Wet oxidation of phenol by hydrogen peroxide using heterogeneous catalysis Fe-ZSM-5: a promising catalyst. *Appl Catal B Environ* 10:L229–L235. doi:10.1016/S0926-3373(96)00041-0

- Hao L, Wang C, Wu Q, Li Z, Zang X, Wang Z (2014) Metal-organic framework derived magnetic nanoporous carbon: novel adsorbent for magnetic solid-phase extraction. *Anal Chem* 86:12199–12205. doi:10.1021/ac5031896
- Hartmann M, Kullmann S, Keller H (2010) Wastewater treatment with heterogeneous Fenton-type catalysts based on porous materials. *J Mater Chem* 20:9002–9017. doi:10.1039/c0jm00577k
- Herney-Ramirez J, Lampinen M, Vicente MA, Costa CA, Madeira LM (2008) Experimental design to optimize the oxidation of Orange II dye solution using a clay-based Fenton-like catalyst. *Ind Eng Chem Res* 47:284–294. doi:10.1021/ie070990y
- Hou L, Zhang Q, Jérôme F, Duprez D, Zhang H, Royer S (2014) Shape-controlled nanostructured magnetite-type materials as highly efficient Fenton catalysts. *Appl Catal B Environ* 144:739–749. doi:10.1016/j.apcatb.2013.07.072
- Kavitha V, Palanivelu K (2016) Degradation of phenol and trichlorophenol by heterogeneous photo-Fenton process using Granular Ferric Hydroxide®: comparison with homogeneous system. *Int J Environ Sci Technol* 13:927–936. doi:10.1007/s13762-015-0922-y
- Lee HJ, Cho W, Lim E, Oh M (2014) One-pot synthesis of magnetic particle-embedded porous carbon composites from metal-organic frameworks and their sorption properties. *Chem Commun* 50:5476–5479. doi:10.1039/c4cc01914h
- Lei Z, Xiao Y, Dang L, You W, Hu G, Zhang J (2007) Nickel-catalyzed fabrication of SiO₂, TiO₂/graphitized carbon, and the resultant graphitized carbon with periodically macroporous structure. *Chem Mater* 19:477–484. doi:10.1021/cm061806m
- Li X, Gai F, Guan B, Zhang Y, Liu Y, Huo Q (2015a) Fe@C core-shell and Fe@C yolk-shell particles for effective removal of 4-chlorophenol. *J Mater Chem A* 3:3988–3994. doi:10.1039/c4ta05915h
- Li X, Liu X, Xu L, Wen Y, Ma J, Wu Z (2015b) Highly dispersed Pd/PdO/Fe₂O₃ nanoparticles in SBA-15 for Fenton-like processes: confinement and synergistic effects. *Appl Catal B Environ* 165:79–86. doi:10.1016/j.apcatb.2014.09.071
- Li H, Zhu J, Xiao P, Zhan Y, Lv K, Wu L, Li M (2016) On the mechanism of oxidative degradation of rhodamine B over LaFeO₃ catalysts supported on silica materials: role of support. *Micropor Mesopor Mater* 221:159–166. doi:10.1016/j.micromeso.2015.09.034
- Liao Q, Sun J, Gao L (2009) Degradation of phenol by heterogeneous Fenton reaction using multi-walled carbon nanotube supported Fe₂O₃ catalysts. *Colloids Surf A Physicochem Eng Asp* 345:95–100. doi:10.1016/j.colsurfa.2009.04.037
- Lin S-S, Gurol MD (1998) Catalytic decomposition of hydrogen peroxide on iron oxide: kinetics, mechanism, and implications. *Environ Sci Technol* 32:1417–1423. doi:10.1021/es970648k
- Liu Y, Xu X, Wang M, Lu T, Sun Z, Pan L (2015) Metal-organic framework-derived porous carbon polyhedra for highly efficient capacitive deionization. *Chem Commun* 51:12020–12023. doi:10.1039/c5cc03999a
- Luo L, Zhang A, Janik MJ, Song C, Guo X (2016) Mesoporous graphitic carbon nitride functionalized iron oxides for promoting phenol oxidation activity. *RSC Adv* 6:91960–91967. doi:10.1039/c6ra19455a
- Lyu L, Zhang L, Wang Q, Nie Y, Hu C (2015) Enhanced Fenton catalytic efficiency of gamma-Cu-Al₂O₃ by sigma-Cu²⁺-ligand complexes from aromatic pollutant degradation. *Environ Sci Technol* 49:8639–8647. doi:10.1021/acs.est.5b00445
- Maldonado-Hódar FJ, Moreno-Castilla C, Rivera-Utrilla J, Hanzawa Y, Yamada Y (2000) Catalytic graphitization of carbon aerogels by transition metals. *Langmuir* 16:4367–4373. doi:10.1021/la991080r
- Martínez F, Calleja G, Melero JA, Molina R (2007) Iron species incorporated over different silica supports for the heterogeneous photo-Fenton oxidation of phenol. *Appl Catal B Environ* 70:452–460. doi:10.1016/j.apcatb.2005.10.034
- Martínez F, Molina R, Pariente MI, Siles JA, Melero JA (2017) Low-cost Fe/SiO₂ catalysts for continuous Fenton processes. *Catal Today* 280:176–183. doi:10.1016/j.cattod.2016.04.044
- Melero JA, Calleja G, Martínez F, Molina R (2006) Nanocomposite of crystalline Fe₂O₃ and CuO particles and mesostructured SBA-15 silica as an active catalyst for wet peroxide oxidation processes. *Catal Commun* 7:478–483. doi:10.1016/j.catcom.2006.01.008
- Melero JA, Calleja G, Martínez F, Molina R, Pariente MI (2007) Nanocomposite Fe₂O₃/SBA-15: an efficient and stable catalyst for the catalytic wet peroxidation of phenolic aqueous solutions. *Chem Eng J* 131:245–256. doi:10.1016/j.cej.2006.12.007
- Nakagawa H, Yamaguchi E (2012) Influence of oxalic acid formed on the degradation of phenol by Fenton reagent. *Chemosphere* 88:183–187. doi:10.1016/j.chemosphere.2012.02.082
- Nidheesh PV (2015) Heterogeneous Fenton catalysts for the abatement of organic pollutants from aqueous solution: a review. *RSC Adv* 5:40552–40577. doi:10.1039/c5ra02023a
- Ribeiro RS, Silva AMT, Figueiredo JL, Faria JL, Gomes HT (2016) Catalytic wet peroxide oxidation: a route towards the application of hybrid magnetic carbon nanocomposites for the degradation of organic pollutants. A review. *Appl Catal B Environ* 187:428–460. doi:10.1016/j.apcatb.2016.01.033
- Santos A, Yustos P, Rodríguez S, Simon E, Romero A (2010) Fenton pretreatment in the catalytic wet oxidation of phenol. *Ind Eng Chem Res* 49:5583–5587. doi:10.1021/ie1004948
- Sashkina KA, Polukhin AV, Labko VS, Ayupov AB, Lysikov AI, Parkhomchuk EV (2016) Fe-silicalites as heterogeneous Fenton-type catalysts for radiocobalt removal from EDTA chelates. *Appl Catal B Environ* 185:353–361. doi:10.1016/j.apcatb.2015.12.038
- Satishkumar G, Landau MV, Buzaglo T, Frimet L, Ferentz M, Vidruk R, Wagner F, Gal Y, Herskowitz M (2013) Fe/SiO₂ heterogeneous Fenton catalyst for continuous catalytic wet peroxide oxidation prepared in situ by grafting of iron released from LaFeO₃. *Appl Catal B Environ* 138–139:276–284. doi:10.1016/j.apcatb.2013.02.040
- Su P, Jiang L, Zhao J, Yan J, Li C, Yang Q (2012) Mesoporous graphitic carbon nanodisks fabricated via catalytic carbonization of coordination polymers. *Chem Commun* 48:8769–8771. doi:10.1039/c2cc34234k
- Tang J, Wang T, Sun X, Guo Y, Xue H, Guo H, Liu M, Zhang X, He J (2013) Effect of transition metal on catalytic graphitization of ordered mesoporous carbon and Pt/metal oxide synergistic electrocatalytic performance. *Micropor Mesopor Mater* 177:105–112. doi:10.1016/j.micromeso.2013.04.027
- Torad NL, Li Y, Ishihara S, Ariga K, Kamachi Y, Lian H-Y, Hamoudi H, Sakka Y, Chaikittisilp W, Wu KCW, Yamauchi Y (2014) MOF-derived nanoporous carbon as intracellular drug delivery carriers. *Chem Lett* 43:717–719. doi:10.1246/cl.131174
- Wang T, Zhao H, Wang H, Liu B, Li C (2016) Research on degradation product and reaction kinetics of membrane electro-bioreactor (MEBR) with catalytic electrodes for high concentration phenol wastewater treatment. *Chemosphere* 155:94–99. doi:10.1016/j.chemosphere.2016.03.140
- Wei X, Wan S, Jiang X, Wang Z, Gao S (2015) Peanut-shell-like porous carbon from nitrogen-containing poly-N-phenylethanolamine for high-performance supercapacitor. *ACS Appl Mater Interfaces* 7:22238–22245. doi:10.1021/acsami.5b05022
- Yang X-j, P-f T, Zhang X-m YX, Wu T, Xu J, Y-f H (2015) The generation of hydroxyl radicals by hydrogen peroxide decomposition on FeOCl/SBA-15 catalysts for phenol degradation. *AICHE J* 61:166–176. doi:10.1002/aic.14625
- Zazo JA, Casas JA, Mohedano AF, Gilarranz MA, Rodríguez JJ (2005) Chemical pathway and kinetics of phenol oxidation by Fenton's reagent. *Environ Sci Technol* 39:9295–9302. doi:10.1021/es050452h

- Zazo JA, Casas JA, Mohedano AF, Rodríguez JJ (2006) Catalytic wet peroxide oxidation of phenol with a Fe/active carbon catalyst. *Appl Catal B Environ* 65:261–268
- Zeng T, Zhang X, Wang S, Ma Y, Niu H, Cai Y (2014) Assembly of a nanoreactor system with confined magnetite core and shell for enhanced Fenton-like catalysis. *Chem Eur J* 20:6474–6481. doi:10.1002/chem.201304221
- Zhang S, Zhao X, Niu H, Shi Y, Cai Y, Jiang G (2009) Superparamagnetic Fe₃O₄ nanoparticles as catalysts for the catalytic oxidation of phenolic and aniline compounds. *J Hazard Mater* 167:560–566. doi:10.1016/j.jhazmat.2009.01.024
- Zhang L, Ye H, Zhao L, Zhang L, Yao L, Zhang Y, Li H (2015) Design of isolated iron species for Fenton reactions: lyophilization beats calcination treatment. *Chem Commun* 51:16936–16939. doi:10.1039/c5cc06590a
- Zheng C, Cheng X, Yang C, Zhang C, Li H, Kan L, Xia J, Sun X (2015) Hydrophilic modification of ordered mesoporous carbon supported Fe nanoparticles with enhanced adsorption and heterogeneous Fenton-like oxidation performance. *RSC Adv* 5:98842–98852. doi:10.1039/c5ra15156b
- Zhou L, Shao Y, Liu J, Ye Z, Zhang H, Ma J, Jia Y, Gao W, Li Y (2014) Preparation and characterization of magnetic porous carbon microspheres for removal of methylene blue by a heterogeneous Fenton reaction. *ACS Appl Mater Interfaces* 6:7275–7285. doi:10.1021/am500576p